

PACS 07.57.Kp, 72.20.Ht

Zero bias terahertz and subterahertz detector operating at room temperature

N. Momot*, V. Zabudsky, Z. Tsybrii, M. Apats'ka, M. Smolii, N. Dmytruk

*V. Lashkaryov Institute of Semiconductor Physics, NAS of Ukraine,
41, prospect Nauky, 03028 Kyiv; e-mail: momotnatasha@isp.kiev.ua*

Abstract. In this paper, the experimental study of the terahertz and subterahertz hot electron bolometer based on narrow-gap semiconductor compound $\text{Hg}_{1-x}\text{Cd}_x\text{Te}$ is presented. The measurements were performed in the temperature range from 77 to 300 K at various operating mode and frequency. The estimated value of the noise equivalent power at room temperature for detector proposed was $1.3 \cdot 10^{-8} \text{ W/Hz}^{1/2}$ and $5.4 \cdot 10^{-9} \text{ W/Hz}^{1/2}$ at bias current $I = 1 \text{ mA}$ and $I = 0$, respectively.

Keywords: THz radiation, bolometer, hot-carrier effect.

Manuscript received 02.02.10; accepted for publication 25.03.10; published online 30.04.10.

1. Introduction

Currently, there is a substantial interest in a part of the spectrum located between microwave and optical ranges. Commonly this frequency band is defined as 0.1-10 THz and called "the terahertz region". The attention to terahertz radiation is caused by its unique properties because of which it finds a wide use for science and technology [1].

Particularly, it is of great interest to create the detection array for terahertz imaging. Heterodyne detectors are the most sensitive in the terahertz region [2], but creating terahertz heterodyne arrays is associated with some difficulties: i) because of all array elements require a common local oscillator, the number of elements is limited of its power; ii) heterodyne terahertz detectors are mainly based on superconductors now (semiconductor-insulator-semiconductor structures or hot electron bolometers) [3] that are in need of cooling to the superconducting transition temperature. Since open-cycle cooling systems are awkward and expensive while closed-cycle cooling systems are low-power, the cryogenic cooling limits the expansion of the number of array elements, too. Therefore, heterodyne terahertz detector arrays are constructed now with a small number of elements (a few tens) [4]. The direct-detection matrix receivers are better in comparison with heterodyne detectors concerning the number of elements expansion.

In this paper, a direct-detection terahertz and subterahertz receiver based on narrow-gap semiconductor compound $\text{Hg}_{1-x}\text{Cd}_x\text{Te}$ (MCT) is

investigated. This detector can operate at room temperature, zero bias and have several micrometers area. Therefore, compact terahertz detector array can be created as based on this material.

2. Design of detector and experimental results

As basic material for manufacturing the THz detector, *p*-type conductivity epitaxial films $\text{Cd}_x\text{Hg}_{1-x}\text{Te}/\text{CdZnTe}$ ($x = 0.22-0.23$) were used. These were grown using liquid phase epitaxy technique providing carrier concentration $3.6 \cdot 10^{15}$ to $2 \cdot 10^{16} \text{ cm}^{-3}$ and thicknesses of layers within the range 2-20 μm . Taking into account the mechanical and electro-physical properties of CdHgTe , the design and technological route of a multi-element detector was developed.

The technological route of manufacturing this structure consists of the following stages:

- control of MCT layers quality by using optical microscopy and IR-Fourier spectroscopy methods;
- preliminary chemical preparation of MCT surface;
- formation of CdTe passivation layer;
- photolithography processes;
- metallization through lift-off photolithography method.

The surface of a detector active element has been protected by CdTe thin film formed using the hot wall epitaxy method. Metallic contacts to the active element, which serve as antenna, have been placed on the passivation layer. Etching the mesa-structures was used (up to the high-resistance substrate) with the purpose of short-circuit prevention between matrix elements. The

electrical contacts between sensitive element and antenna have been realized by chemical etching the contact windows into the passivation layer. Special bromic etchant has been picked up for etching these passivation thin layers.

The detector matrix consists of 4×11 elements (each of it has $10 \times 50 \mu\text{m}^2$ active area and was connected to the bow-tie like antenna with $568750 \mu\text{m}^2$ area). The scheme and microphoto of the detector with antenna are shown in Fig. 1.

The theory of the photoresponse mechanism of such detector has been proposed in [5]. In this device, the radiation heats electrons in the semiconductor, whereas semiconductor lattice heating is absent. The heating changes generation-recombination processes that produce changes of the carrier number and of the semiconductor resistance. A value of the semiconductor hot electron bolometer response time is determined by the carrier lifetime.

The response of $\text{Hg}_{1-x}\text{Cd}_x\text{Te}$ bolometer was measured in the range of frequencies 0.037-1.58 THz and in the temperature range from 77 to 300 K at various detector bias currents. The experimental results indicating that the detector is sensitive in the mentioned range are presented in [6]. In addition, these results show that the photoresponse of p -type $\text{Hg}_{1-x}\text{Cd}_x\text{Te}$ at zero bias is higher than that of the n -type $\text{Hg}_{1-x}\text{Cd}_x\text{Te}$.

In Fig. 2, the response of p -type MCT bolometer is shown as the function of temperature for the acceptor concentration $N_p = 7 \cdot 10^{15} \text{cm}^{-3}$, mole fraction of CdTe $x = 0.2$ and dimensions of the sensitive element $10 \times 50 \times 17 \mu\text{m}$. At $T = 77 \text{ K}$ the value of photoresponse at non-zero bias is several times higher than at $I = 0$ for that sample. At the same time, at room temperature the value of photoresponse is of the same order of magnitude for $I = 1 \text{ mA}$ and $I = 0$.

Fig. 3 demonstrates the photoresponse of this bolometer as the function of the detector current. The deviation from linearity at close to zero biases is probably caused by rectifying effect between semiconductor and metallization. For example, in Fig. 4 the experimental results for another sample response as the function of detector current at $T = 77 \text{ K}$ and its $I - V$ characteristic are presented. For this sample, the detector sensitivity at zero bias current even higher as compared to the non-zero bias.

As a rule, to characterize THz detectors, the noise equivalent power (NEP) is used. NEP is the radiant power needed to generate signal equivalent to noise. The NEP can be calculated as:

$$\text{NEP} = \frac{U_N}{S_V (\Delta f)^{1/2}}, \quad (1)$$

where U_N is the noise voltage, S_V – detector voltage sensitivity, Δf – pass bandwidth.

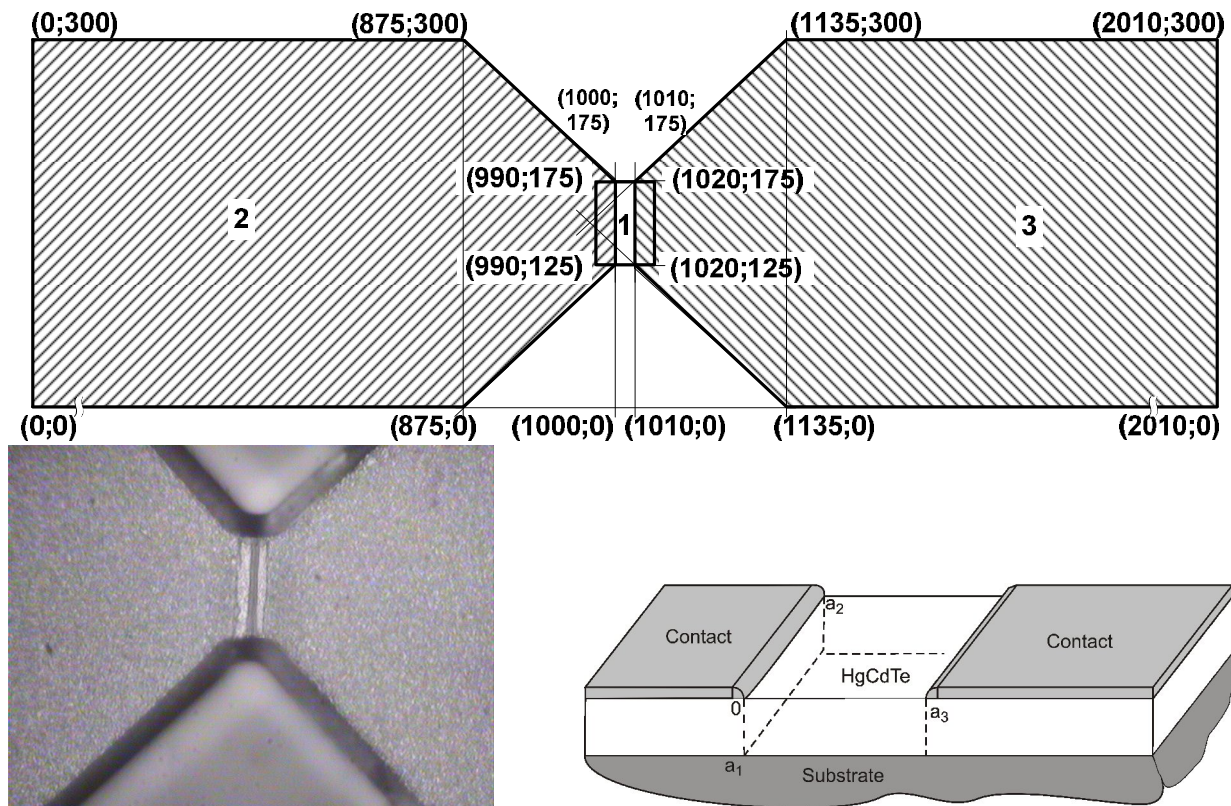


Fig. 1. Scheme of THz antenna and microphoto of its central part that were made using high resolution optical microscopy. The area 1 is the active element, 2 and 3 – metallic contacts.

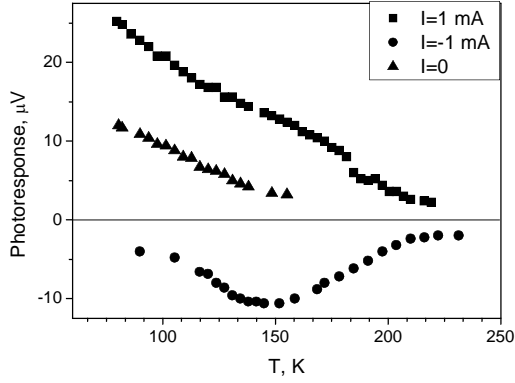


Fig. 2. The bolometer response as a function of temperature. The frequency of incident radiation is $\nu = 78$ GHz. The frequency of modulation is $\Delta f = 360$ Hz. The radiation flux density is ~ 4.5 mW/cm² in the place of sample location.

Cd_xHg_{1-x}Te photoresistors are typically characterized with the Johnson noise, generation-recombination noise, and photon noise.

The mean-square power for Johnson's noise is [7]:

$$\langle U_J \rangle^2 = 4Rk_B T \Delta f, \quad (2)$$

where R is the sample resistance, k_B is the Boltzmann constant, T is sample temperature, Δf is a bandwidth for the central frequency.

The spectral density of generation-recombination noise current caused by interband transitions is of the form [8]:

$$S_I(f) = \frac{4I_c^2 (b+1)^2 n_0 p_0 \tau}{(bn_0 + p_0)^2 (n_0 + p_0) (1 + \omega^2 \tau^2)}, \quad (3)$$

where $b = \mu_n / \mu_p$ is the mobility ratio, τ is the dominant lifetime, I_c is the current, n_0 and p_0 refer to the total numbers of electrons and holes in the sample of thermal equilibrium. The generation-recombination noise voltage is equal

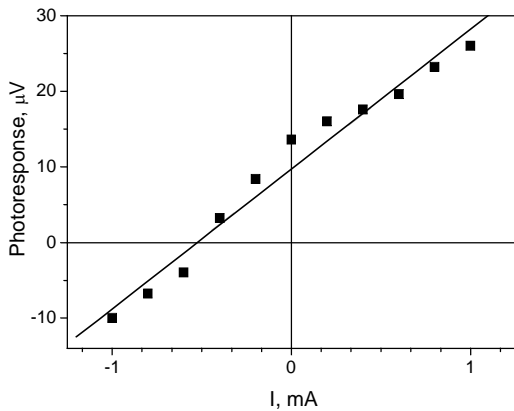


Fig. 3. The bolometer response as a function of detector current at $T = 77$ K. The frequency of incident radiation is $\nu = 78$ GHz. The frequency of modulation is $\Delta f = 360$ Hz. The radiation flux density is ~ 4.5 mW/cm² in the place of sample location.

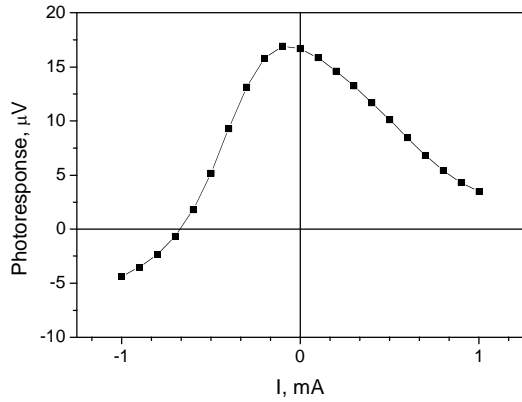
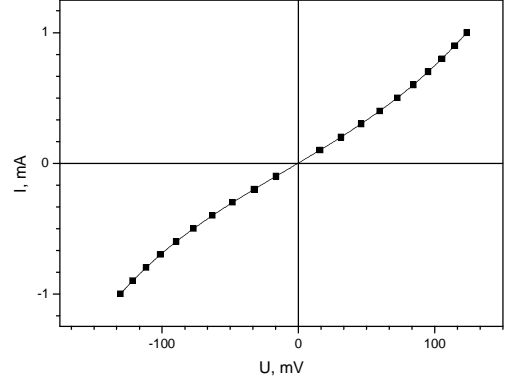


Fig. 4. The I - V characteristic and bolometer response as a function of detector current at $T = 77$ K. The frequency of incident radiation is $\nu = 130$ GHz.

$$\langle U_{g-r} \rangle^2 = S_I R^2 \Delta f. \quad (4)$$

For photon noise (the dispersion of falling to sample photons number), the next expression can be written [9]

$$U_{phn} = (2A\eta \langle N \rangle)^{1/2} eR, \quad (5)$$

where N is the photon flux from the $T = 300$ K background hemisphere, e is the electron charge, $\eta = 0.5$ is the quantum efficiency of detector, and A is the sensitive element area.

$$N(T) = \int_{\lambda_1}^{\lambda_2} \frac{2\pi c}{\lambda^4 \left(e^{\frac{hc}{\lambda kT}} - 1 \right)} d\lambda. \quad (6)$$

General noise is estimated using the following formula:

$$U = \sqrt{U_{g-r}^2 + U_J^2 + U_{phn}^2}. \quad (7)$$

The noise voltages in the sample were estimated from Eqs (2)-(7) at $\Delta f = 1$ Hz and the results have been summarized in Table 1.

At room temperature, generation-recombination noise is higher than the other ones. Because of the generation-recombination noise is apparent at the current flow through the sample, its contribution can be excluded by a zero bias mode.

Table 1. Estimated noise voltages.

Noise type	$T = 77 \text{ K}$	$T = 300 \text{ K}$
Johnson's noise	$5.1 \cdot 10^{-10} \text{ V}$	$5.4 \cdot 10^{-10} \text{ V}$
Generation-recombination noise	$2 \cdot 10^{-11} \text{ V}$	$1.2 \cdot 10^{-9} \text{ V}$
Photon noise	$1.4 \cdot 10^{-11} \text{ V}$	$1.7 \cdot 10^{-12} \text{ V}$

Given in Table 2 are the values of estimated noise equivalent power for the detector currents $I = 1 \text{ mA}$ and $I = 0$.

Table 2. Estimated NEP.

	Detector current, I	$T = 77 \text{ K}$	$T = 300 \text{ K}$
NEP, $\text{W/Hz}^{1/2}$	1 mA	$4 \cdot 10^{-10}$	$1.3 \cdot 10^{-8}$
	0	$8 \cdot 10^{-10}$	$5.4 \cdot 10^{-9}$

Thus, because of the smaller noise, the detector threshold sensitivity is higher at zero bias than at an applied current despite a smaller photoresponse. The estimated noise equivalent power of detector is comparable with the NEP of other terahertz uncooled devices [10, 11].

3. Conclusions

The semiconductor hot electron bolometer based on narrow-gap $\text{Hg}_{1-x}\text{Cd}_x\text{Te}$ can be used for detection of terahertz and subterahertz radiation. The noise equivalent power of such detector that operates at room temperature and zero bias is of the order of $10^{-9} \text{ W/Hz}^{1/2}$, thus multi-element terahertz detector can be created as being based on it.

References

1. F P. Siegel, Terahertz technology // *IEEE Trans. Microwave Theory and Techniques* **50**(3), p. 910-928 (2002).
2. F. Sizov, THz radiation sensors // *Opto-Electron. Rev.* **18**(1), p. 10-36 (2010).
3. Sheng-Cai Shi, Superconducting THz detectors and their applications in radio astronomy // *Terahertz Science and Technology* **1**(4), p. 199-215 (2008).
4. I.I. Eru, Matrix multibeam reception of submillimeter and infrared electromagnetic waves (the state-of-the-art and trends) // *Radio Physics and Radio Astronomy* **11**(3), p. 298-307 (2006).
5. V. Dobrovolsky, F. Sizov, A room temperature, or moderately cooled, fast THz semiconductor hot electron bolometer // *Semicond. Sci. Technol.* **22**, p. 103-106 (2007).
6. F.F. Sizov, V. Dobrovolsky, V. Zabudsky, Yu. Kamenev, N. Momot, and J. Gumenjuk-Sychevska, mm- and THz-waves detector on the base of narrow-gap semiconductors // *Proc. SPIE* **7309** (2009).
7. N.B. Lukyanchikova, *Noise Research in Semiconductor Physics*. Gordon and Breach Science Publishers, Amsterdam, 1999.
8. R.N. Sharma, K.M. van Vliet, Generation-recombination fluctuations in mercury-cadmium telluride // *Phys. status solidi (a)* **1**, p. 765-773 (1970).
9. A. van der Ziel, *Noise in Measurements*. John Wiley & Sons Inc., 1976.
10. El Fatimy, A. Delagnes, J.C. Younus, A. Nguema, E. Teppe, F. Knap, W. Abraham, E. Mounaix, Plasma wave field effect transistor as a resonant detector for 1 terahertz imaging applications // *Optics Communs* **282**(15), p. 3055-3058 (2009).
11. J.L. Hesler, T.W. Crowe, Responsivity and noise measurements of zero-bias Schottky diode detectors // 18th Intern. Symp. Space Terahertz Techn., Pasadena, 2007.